coatings

MDPI

Review

Dopants for Enhanced Performance of Tin-Based Perovskite Solar Cells—A Short Review

Hairui Liu [1], Zuhong Zhang [1], Feng Yang [2,*], Jien Yang [1], Andrews Nirmala Grace [3], Junming Li [4,*], Sapana Tripathi [5] and Sagar M. Jain [6,*]

1 College of Material Science and Engineering, Henan Normal University, Xinxiang 453007, China; liuhairui1@126.com (H.L.); zhangzuhong0413@163.com (Z.Z.); yjen@htu.cn (J.Y.)
2 Henan Key Laboratory of Photovoltaic Material, School of Physics, Henan Normal University, Xinxiang 453007, China
3 Centre for Nanotechnology Research, Vellore Institute of Technology, Vellore 632014, India; anirmalagrace@vit.ac.in
4 Fujian Provincial Key Laboratory of Electrochemical Energy Storage Materials, Fuzhou University, Fuzhou 350002, China
5 Department Magnetic Materials, Max Planck Institute for Intelligent Systems, Heisenbergstraße 3, 70569 Stuttgart, Germany; sapana.t15@gmail.com
6 Photovoltaics and Optoelectronics Laboratory, Center for Renewable Energy Systems, School of Water, Energy and Environment, Cranfield University, Cranfield, Bedfordshire MK43 0AL, UK
* Correspondence: yangfeng@htu.edu.cn (F.Y.); li@bistu.edu.cn (J.L.); Sagar.M.Jain@cranfield.ac.uk (S.M.J.)

Abstract: Lead-based perovskite solar cells had reached a bottleneck and demonstrated significant power conversion efficiency (PCE) growth matching the performance of traditional polycrystalline silicon solar cells. Lead-containing perovskite solar cell technology is on the verge of commercialization and has huge potential to replace silicon solar cells, but despite the very promising future of these perovskite solar cells, the presence of water-soluble toxic lead content is a growing concern in the scientific community and a major bottleneck for their commercialization. The less toxic, tin-based perovskite solar cells are promising alternatives for lead-free perovskite solar cells. Like lead-based perovskite, the general chemical formula composition of tin-based perovskite is $ASnX_3$, where A is a cation and X is an anion (halogen). It is evident that tin-based perovskites, being less-toxic with excellent photoelectric properties, show respectable performance. Recently, numerous studies reported on the fabrication of Sn-based perovskite solar cells. However, the stability of this novel lead-free alternative material remains a big concern. One of the many ways to stabilize these solar cells includes addition of dopants. In this context, this article summarizes the most important fabrication routes employing dopants that have shown excellent stability for tin-based perovskite photovoltaics and elaborates the prospects of lead-free, tin based stable perovskite photovoltaics.

Keywords: lead-free; tin-based; perovskite solar cells

Citation: Liu, H.; Zhang, Z.; Yang, F.; Yang, J.; Grace, A.N.; Li, J.; Tripathi, S.; Jain, S.M. Dopants for Enhanced Performance of Tin-Based Perovskite Solar Cells—A Short Review. *Coatings* **2021**, *11*, 1045. https://doi.org/10.3390/coatings11091045

Academic Editors: Alessandro Latini and Francesco Di Quarto

Received: 4 August 2021
Accepted: 27 August 2021
Published: 30 August 2021

1. Introduction

Lead-based perovskite solar cells have been in the limelight of solar cell devices for more than a decade, and their power conversion efficiency (PCE) has grown rapidly from 3.80% (year 2009) to 25.50% (year 2020) [1,2]. The absorption layers of traditional lead-based perovskite solar cells possess an $APbX_3$ configuration, where A refers to a metal cation or organic cation such as monovalent cesium cation (Cs^+), methylammonium (CH_3NH_3, MA^+), formamidinium (NH_2CHNH_2, FA^+) and so on; X is the halogen anion, such as iodide (I^-), bromide (Br^-), chloride (Cl^-), or a combination of the above halogens [3]. Since the last decade, there are intriguing research studies worldwide on lead-based perovskite solar cells. There exists a wide range of variety and flexibility in perovskite solar cells like fine tuning the perovskite composition [4–7], types of additives [8–10], structure [11,12], employing different electron transport or hole transport layers [13,14]. There is a significant

development in PCE and stability of perovskite solar cells and many commercial companies across the world are investing heavily in the manufacture of these 3rd generation solar cells. A few to mentions are Oxford PV GmbH (Brandenburg, Germany); Saule Technology (Wroclaw, Poland); Microquanta Semiconductor (Hangzhou, China); Solaronix (Aubonne, Switzerland); Swiftsolar (Sancarlos, CA, USA), etc. However, the highly toxic lead metal present in these solar cells still remains a major environmental concern [15] as the recycling of such a heavy metal is complicated and expensive. Therefore, researchers have been looking for metal ions that can replace lead in perovskite materials. The radius must not be too different from that of lead ions (Pb^{2+}), otherwise the replacement will cause lattice distortion and form defects. In the periodic table, Sn, located in the same main group as Pb and presenting a close atomic radius, has attracted huge attention from the scientific community. The ionic radius of Pb^{2+} is 119 pm and that of Sn^{2+} is 118 pm, which allows the simple replacement of Pb by Sn in tin-based perovskite solar cells [16]. However, tin suffers from the notorious problem of easily being oxidized from Sn^{2+} to Sn^{4+} on exposure to ambient conditions [17–20]. This stability concern remains a challenge for long lasting stability of tin-based perovskite cells.

Studies showed that tetravalent tin ion (Sn^{4+}) is self-doped during the crystallization process of perovskite, and it was concluded that the homogeneous distribution of a small amount of Sn^{4+} could increase the conductivity of perovskite solar cells [21]. However, an excessive amount of Sn^{4+} could increase the defects of tin-based perovskite, which could degrade the performance of perovskite solar cells [17,22,23]. Since the first report of pure tin-based perovskite solar cells in 2014 [17], research on pure tin-based perovskite solar cells has become more and more popular with scientific researchers. $FASnI_3$ ($FA=CN_2H_5$) tin-based perovskite is one of many tin-based perovskites, which is an upgraded version of the $MASnI_3$ ($MA=CH_3NH_3$) perovskite type. The former has better thermal stability than the latter [22,23] due to the higher thermal stability of CN_2H_5 compared to CH_3NH_3. Tin-based perovskite solar cells are achieving good efficiency performance and are the closest candidate among the other Pb-free alternatives to compete with lead-based perovskite. Tin-perovskites are generally having low energy bandgaps, such as $MASnI_3$ (1.30 eV), $CsSnI_3$ (1.30 eV) and $FASnI_3$ (1.41 eV) with bandgaps lower than $MAPbI_3$ (1.59 eV) maximizing the absorption of photons from sunlight [24–26]. In 2014, Noel et al., demonstrated the fabrication of $MASnI_3$ perovskite solar cells yielding a PCE of 6.40% for the first time [17]. However, $MASnX_3$ (X=Cl, Br, I) is very unstable in an ambient atmosphere [17]. Considering this drawback in subsequent years, several attempts are made to enhance the efficiency of the more stable $FASnI_3$ and $CsSnI_3$ active material in solar cells, but no improvement in PCE was observed.

One of the most promising approachs to improve the stability of Sn-based perovskite solar cells is the addition of dopants to the tin perovskite material to enhance the homogeneous deposition and to enhance the optoelectronic properties of the absorber layer. Song et al. reported the use of an excess of SnI_2 in $CsSnI_3$ with a PCE of 4.81% [25]. It is demonstrated that the excess of SnI_2 was beneficial to form a uniform film and suppress Sn^{4+} vacancies, thereby reducing the p-type conductivity of tin-based perovskite materials. It was also reported that the combination of SnF_2 and pyrazine solves the problem of perovskite phase aggregation and improves the oxidation resistance of the film [26,27]. In 2016, Chen et al., employed quantum rods (QR) of $CsSnI_3$ to enhance the PCEs of $CsSnI_3$ perovskite solar cells to 12.96% [28].

In 2018, Jokar et al., reported a high PCE of 9.60%. This improved efficiency was the result of using a new Sn-based absorber layer $GA_xFA_{1-x-2}ySnI_{3-y}EDAI_2$, where GA is guanidinium and FA is formamide and $EDAI_2$ is an additive, ethylene diammonium diiodide [29]. Very recently, in 2020, Nishimura et al., fabricated Sn-based perovskite solar cells with a GeI_2 doped $(FA_{0.9}EA_{0.1})_{0.98}EDA_{0.01}SnI_3$ composition as the light-absorbing layer, that reached the highest reported performance so far, a PCE of 13.24% [30]. This enhanced efficiency was the result of the excellent optoelectronic properties of the new absorber layer.

This article summarizes important contributions made by scientific researchers to the development of tin-based perovskite in terms of additives, dimensions, structure and proposes possible future development directions for tin-based perovskites.

2. Additive Engineering

2.1. Inorganic Materials

One of the most important strategies for sustaining the stability of Sn-based perovskite solar cells is by reducing the Sn^{4+} to Sn^{2+}. In this direction, Cao et al., reported that ammonium hypophosphite (AHP, $NH_4H_2PO_2$) could inhibit the oxidation of Sn^{2+}, H_2PO^{2-} acts as a reducing agent that converts Sn^{4+} and inhibits the oxidation of Sn^{2+}. It was observed that addition of AHP to the Sn-perovskite precursor solution enables growth of large perovskite crystals. Further in this study a more stable CuSCN hole transport material was employed, which resulted in the fabrication of a more stable and efficient tin-based perovskite solar cell [31]. Figure 1a,b presents the optoelectronic characterization of an AHP-modified Sn-based perovskite solar cell. Tai and co-workers mixed hydroxybenzene sulfonic acid with $SnCl_2$ to form a composite. When employed in solar cells, this composite could well prevent oxygen from entering the tin-based perovskite film resulting in an enhancement in the stability of the material. Additionally, a highly homogeneous perovskite film was obtained [32]. Figure 1c,d present the performance of the devices prepared following this strategy. Kayesh et al., introduced hydrazinium chloride (N_2H_5Cl) into Sn-perovskite films as a co-additive with SnF_2 to control the uniform growth of the crystals and inhibit the oxidation of Sn^{2+}. The open circuit voltage (Voc) was 0.455 V, short-circuit current density (Jsc) was 17.64 mA cm^{-2}, and energy conversion efficiency (PCE) was 5.4% [33]; the device performance is shown in Figure 1e,f. As a common additive, SnF_2 had been studied by numerous scholars [26,34–41]. Liao and co-workers mixed SnF_2 with diethyl ether to make 5%, 10%, 15%, 20% and 30% gradient antisolvents, of which the optimum 10% of antisolvent produced $FASnI_3$ perovskite films with enhanced homogeneity and coverage. The device reached a PCE of 6.22% [37]. Lee and co-workers found that SnF_2 could form a complex with pyrazine and this complex could play an important role in forming dense and stable perovskite films. The improved performance of perovskite films employing SnF_2-pyrazine complex absorber is shown in Figure 1g. Another research direction is to dope metal cations into organotin-based perovskite materials to study the performance changes of tin-based perovskites. Gao and his collaborators studied the effect of metallic Cs on $FASnI_3$-type perovskite solar cells. They found that Cs doped with monovalent cation sites could play a role in shrinking the lattice, improved the symmetry of perovskite crystals and inhibited the oxidation of Sn^{2+}. After doping with Cs^+, the efficiency of the device had increased by more than 60%, the PCE of the controlled device was 3.74% and the PCE of the doped device was 6.08%. Not only that, but its stability was improved greatly. After being stored in the glove box for 2000 h, the PCE decline was only 10% of the original PCE [42].

2.2. Organic Materials

Organic cations are common and intensively studied additives. Ke and coworkers studied propylenediammonium (PN) and trimethylenediammonium (TN). These two cations influenced $FASnI_3$ perovskite solar cells. The reason is that the two cations could reduce the dimensions of the tin-based perovskite and could form a three-dimensional tin-based perovskite structure, filling the vacancies of SnI_2 in 3D tin-based perovskite crystals.

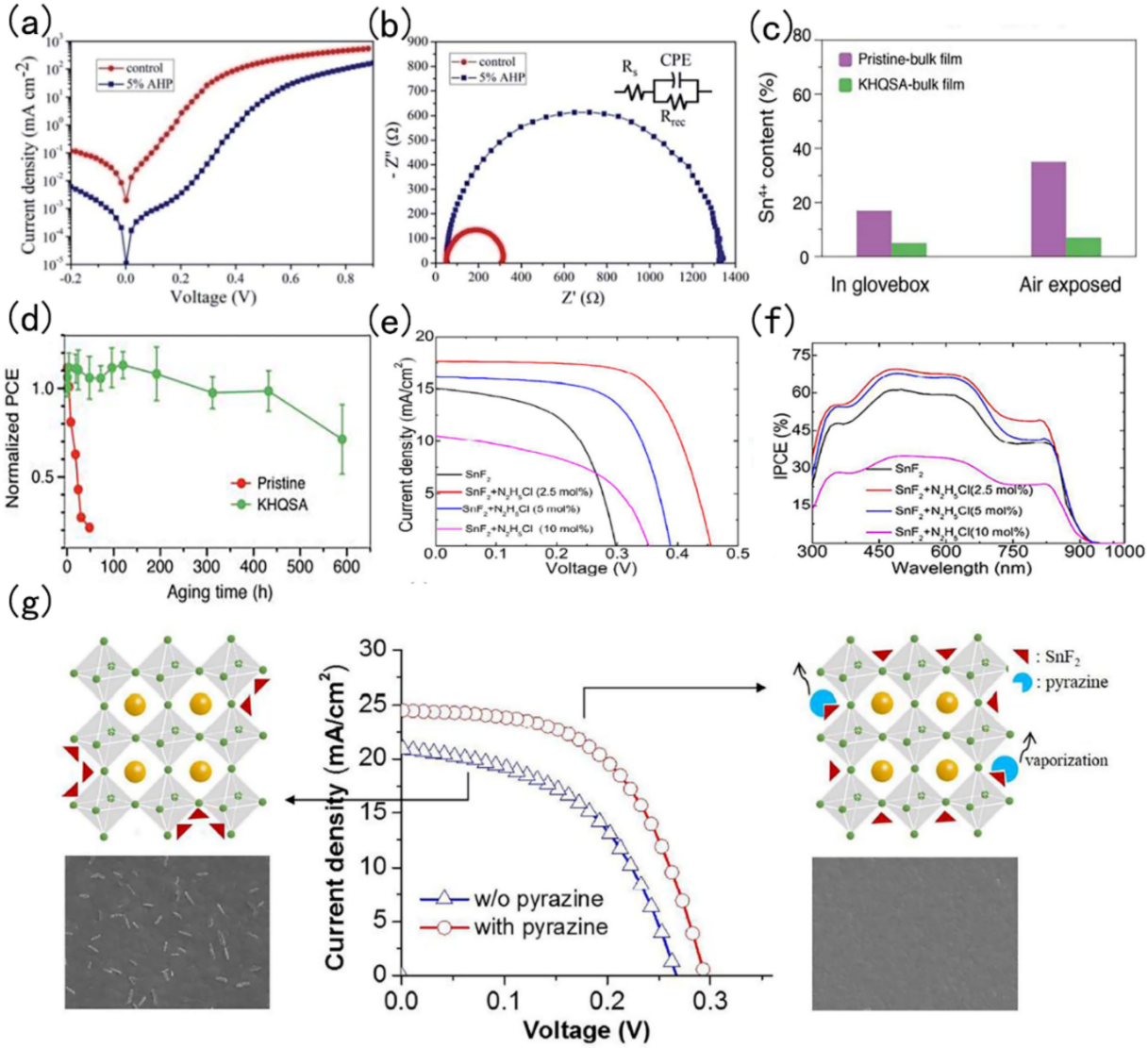

Figure 1. (**a**) J-V curves of $FASnI_3$ solar cells with and without AHP (measured in the dark). Reproduced with permission from [31]. Copyright 2019 Royal Society of Chemistry. (**b**) Nyquist plots of $FASnI_3$ solar cells with and without AHP (inset shows the equivalent circuit for fitting. Reproduced with permission from [31]. Copyright 2019 Royal Society of Chemistry. (**c**) The content of Sn^{4+} in the original perovskite film and the perovskite film with KHQSA were tested in the glove box and the air environment. Reproduced with permission from [32]. Copyright 2019 John Wiley & Sons—Books. (**d**) Stability of the pristine and KHQSA-modified solar cells upon exposure in the dark air (RH = ~20%) without device encapsulation. Reproduced with permission from [32]. Copyright 2019 John Wiley & Sons—Books. (**e**) A comparison of J-V curves. Reproduced with permission from [33]. Copyright 2018 American Chemical Society. (**f**) A comparison of incident photon-to-electron conversion efficiency (IPCE) change with wavelength. Reproduced with permission from [33]. Copyright 2018 American Chemical Society. (**g**) Comparison of J-V curves of doped pyrazine devices and J-V curves of undoped pyrazine devices and comparison of pyrazine acting on perovskite crystals. Reproduced with permission from [26]. Copyright 2016 American Chemical Society.

A perovskite film obtained by adding a mixed solution of PN and FAI in a mixing ratio of 0.1:1 to the precursor solution showed a PCE of 5.85%, while the mixing of TN and FAI in ratio 0.1:1 leads to a device PCE of 5.53%. The PCE of the device after compounding organic cations was thus twice that of the original device (2.53%) [43]. The position and function of PN/TN in the perovskite crystal structure are shown in Figure 2a. Jokar and coworkers studied ethylenediammonium diiodide ($EDAI_2$) and butylammonium iodide (BAI) in $FASnI_3$ perovskite solar cells. They found that the cation BAI could help improve the quality

of the perovskite film, and the cation $EDAI_2$ produced a significant improvement on the perovskite film, providing a good quality perovskite film [44]. The device PCE could reach 8.9%. The position and function of BA^+ and EDA^+ in the perovskite crystal structure are shown in Figure 2b. Kayesh and co-workers studied the addition of 5-ammonium valeric acid iodide (5-AVAI) to the tin-based perovskite and obtained a substantial PCE of 7% for a perovskite solar cell with an area of 0.25 cm^2. 5-AVAI could form hydrogen bonds with I^- or SnI_6^{4-}, thereby regulating the crystal growth direction [45]. Additionally, addition of 5-AVAI improved the solar cell stability. The results are presented in Figure 2c. Ran et al., employed a conjugated large-volume amine (LVA), 3-phenyl-2-propen-1-amine (PPA), PPA could be well compounded with $FASnI_3$, which could improve the random orientation of crystal grains during the formation of thin films, reduce the existence of defects, improve the structural instability, and increase the extraction capacity of excitons. Thus, a high-quality perovskite film was obtained, and a champion device with PCE of 9.61% was obtained. Figure 2d shows the structural formula of PPA and its effect on $FASnI_3$ crystals [46]. Yu and collaborators proposed 2,2,2-trifluoroethylamine hydrochloride (TFEACl). This organic substance is characterized by $TFEA^+$ and Cl^-, which are easy to separate. When added to the precursor solution, $FASnI_{3-x}Cl_x$ was easily formed, which improves the quality of the perovskite morphology. Obviously, the improved valence band of the tin-based perovskite material was better matched with PEDOT: PSS and the conduction band is better matched with the conduction band of PCBM, which could better improve the carrier mobility and enhance device performance [47]. 4-Fluorobenzohydrazide (FBH) was proposed by Him and collaborators. This additive could form a protective film on the surface of perovskite and improve the stability of the device. Under the condition of 0.1 ppm oxygen, the device PCE reaching 9.47%, and the device efficiency was 9.03% in a 100-ppm oxygen environment [48]. FBH was added to the fabrication flow chart of perovskite films is shown in Figure 2e and the morphologies under a scanning electron microscope of perovskite films under different conditions is shown in Figure 2f. Boehm and co-workers employed surface ligands to study the performance of $FASnI_3$ perovskite solar cells. They tested octanoic acid (OCA), trimethylphenyl ammonium chloride (TMPACl), 2*H*,2*H*,3*H*,3*H*-perfluorononanoic acid (FNCA), all of which influenced the performance of the period, of which FNCA had the greatest impact on the device, which could improve the stability of the period [49]. Zeng et al., studied poly(α-methylstyrene) (PAMS). They added different concentrations of PAMS to diethyl ether to form an anti-solvent and cleaned the perovskite film during the spin coating process, which reduced the needle hole-ground effect, which in turn could enhance the adhesion between PCBM and perovskite layer and improve the performance of the device [50]. Meng and colleagues studied the mechanism of effect of poly (vinyl alcohol) (PVA) on $FASnI_3$ and found that the strong hydrogen bonds iPVA could react with $FASnI_3$, which could passivate defects, form a dense film and prevent the diffusion of I^-, the V_{oc} increased by 0.08 eV (0.55 eV to 0.63 eV) and the device efficiency reached 8.9% [51]. Lin and co-workers introduced 8-hydroxyquinoline (8-HQ). They found that the oxygen and nitrogen atoms in HQ could form co-ordination bonds with Sn^{2+} and inhibit the oxidation of Sn^{2+} to Sn^{4+} [52]. Wu and his collaborators studied π-conjugated Lewis bases and synthesized 2-cyano-3-[5-(2,4-difluorophenyl)-2-thienyl]-propenoic acid (CTA-F), 2-cyano-3-[5-(2, dimethoxyphenyl)-2-thienyl]-propenoic acid (CTA-OMe) and 2-cyano-3-[5-[4-(diphenylamino) phenyl]-2-thienyl]-propenoic acid (CDTA). These three substances could form intermediate adducts and coordinate with Sn^{2+} to inhibit the co-crystallization rate of perovskite, thereby optimizing the surface morphology of the perovskite [53].

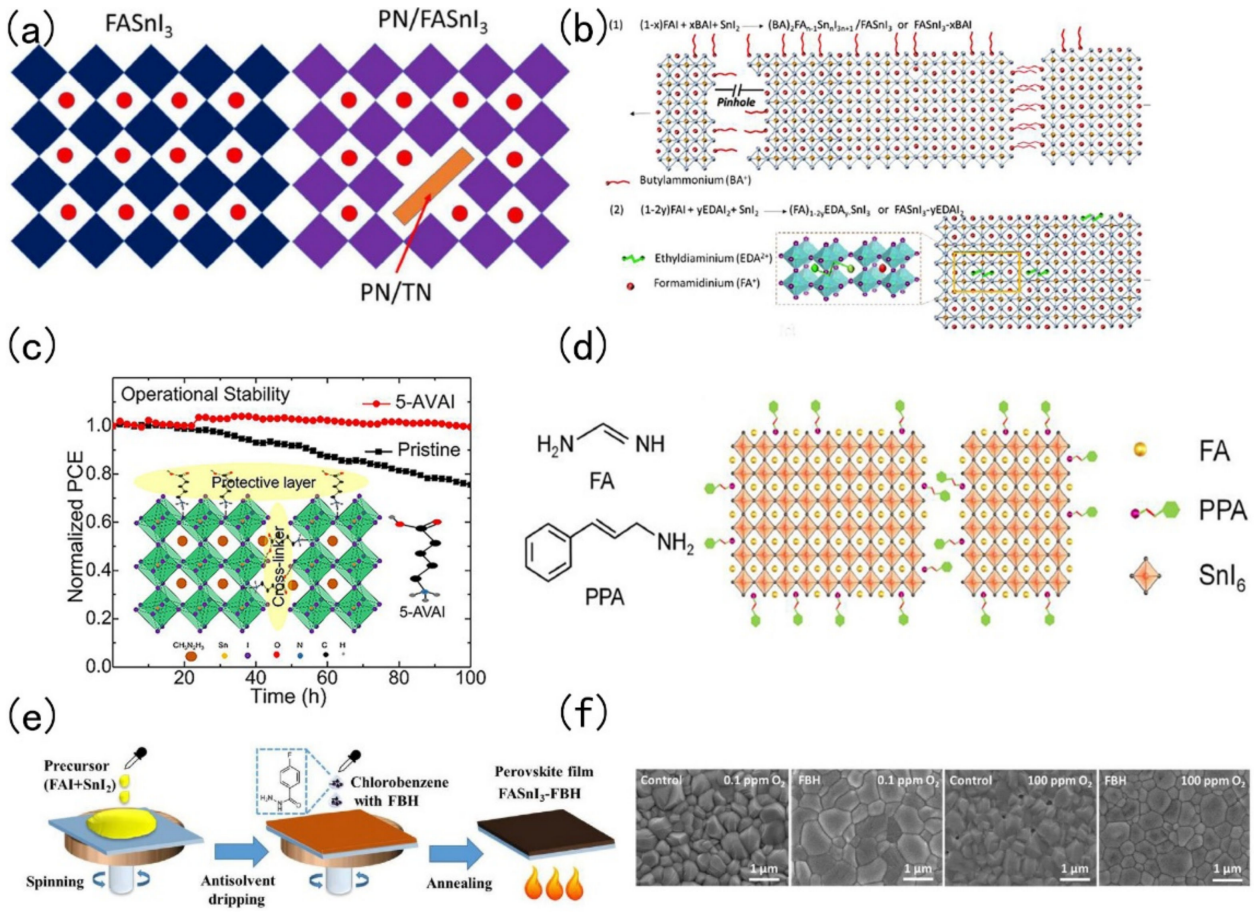

Figure 2. (**a**) Internal structure of PN/TN acting on perovskite). Reproduced with permission from [38]. Copyright 2016 American Chemical Society. (**b**) Internal structure of BA^+/EDA^+ acting on perovskite. Reproduced with permission from [44]. Copyright 2018 The Royal Society of Chemistry. (**c**) The stability of the device with 5-AVAI modification over time and the stability of the device without 5-AVAI modification with time (inside is the diagram of the internal structure of 5-AVAI acting on perovskite). Reproduced with permission from [45]. Copyright 2019 American Chemical Society. (**d**) The chemical structure formula of FA/PPA and the internal structure of PPA acting on perovskite. Reproduced with permission from [46]. Copyright 2019 Elsevier Inc. (**e**) Flow chart of FBH modified perovskite films. Reproduced with permission from [48] Copyright 2020 The Royal Society of Chemistry. (**f**) Scanning electron microscopy image of perovskite film made with/without FBH under different oxygen conditions. Reproduced with permission from [48] Copyright 2020 The Royal Society of Chemistry.

3. Crystal Structure Engineering

Low-dimensional $FASnI_3$ perovskite is a hot spot in current research. The added advantages of low-dimensional tin-based perovskite are its excellent stability, adjustable band gap and excellent photoelectric properties. In 2017, Liao et al., introduced phenylethyl ammonium iodide (PEAI) into a $FASnI_3$ perovskite. PEA could divide the body type perovskite into a 2D structure. This 2D structure was more stable than the 3D structure [54]. The change of perovskite structure with different PEAI levels is shown in Figure 3a. The same year, Ke et al., demonstrated the addition of ethylene diammonium (en) to $FASnI_3$ perovskite. The 3D $FASnI_3$ type perovskite had an adjustable structure, mainly because $\{en\}FASnI_3$ could generate many Schottky defects in the crystal structure. Schottky defects provide to ability to change the bandgap of tin-based perovskite [55]. The crystal diagram is shown in Figure 3b. Ran et al., used a multi-channel diffusion two-step film formation method. In this process, phenylethyl ammonium iodide (PEAI) was evaporated to the surface of FAI and then SnI_2 is evaporated to form a 2D-3D heterojunction perovskite material. This 2D-3D structure could improve the quality and the photoelectric performance

of the film. The fabricated device employing this 2D-3D tin-based perovskite structure achieved a PCE of 6.98% [56]. The 2D-3D heterojunction fabrication flow chart is shown in Figure 3c. Ng and co-workers added PEAI and Ge in $FASnI_3$, where PEAI mainly plays a role of blocking water and Ge could reduce the reduce density of trap states in the perovskite [57]. The roles and positions of Ge^{2+} and PEA^+ in perovskite crystals are shown in Figure 3d. Wang and co-workers fabricated a 2D-quasi-2D-3D Sn perovskite film with the pseudohalogen ammonium thiocyanate (NH_4SCN). The film had good oxidation resistance that enhanced the stability of the resulting perovskite film [58]. Structure characterization of the control film and structure characterization of film with HSP (2D-quasi-2D-3D structure) are shown in Figure 3e.

In 2018, Xu et al., employed 5-ammonium valeric acid (5-AVA) and NH_4Cl to make quasi-2D perovskites. The perovskite crystals had a vertical orientation that minimises recombination. They found that NH_4Cl plays an important catalytic role in the crystal growth direction. Such vertically oriented grains were conducive to the migration of the charge carrier, thereby improving the performance of the solar cell [60]. Tsai et al., found that different proportions of 2-hydroxyethylammonium (HEA^+) ion mixed with FA^+ could change the dimensions of perovskite crystals. Below 100%, it formed a 3D orthogonal structure; at 100%, it was a 2D orthogonal structure [61]. In 2020, Li and co-workers encapsulated the perovskite layer, where they introduced butylethylammonium (BEA) and synthesized perovskite of $(BEA)(FA)_{n-1}SnnI_{3n+1}$ (n = 1–3) with a low-dimension Dion-Jacobson phase. The advantage of the tin-based perovskite of this material and low-dimensional tin-based perovskite was that its band gap was less affected by lattice distortion. Moreover, the low-dimensional tin-based perovskite was stable against attack by water and oxygen. Due to the introduction of BEA the confinement effect of quantum wells was also greatly reduced, and the migration length of carriers reaches 340 nm (holes) and 450 nm (electrons) [62]. In the same year, Li et al., synthesized a vertically oriented 2D tin-based perovskite. They introduced phenylethylammonium chloride (PEACl) to grow a vertically oriented 2D tin-based perovskite. Usual parallel oriented 2D perovskite has good stability but negatively affects the electrical properties due to the fact large-long alkyl chain cations will hinder the carrier transportation [63]. On the contrary, the vertically oriented 2D tin-based perovskite $FASnI_3$: PEACl demonstrated an improved stability with the photoelectric performance reaching 9%, but the growth of this 2D tin-based perovskite was highly temperature sensitive at only 100 °C, and then the film was pure vertical 2D tin-based perovskite [59]. Figure 3f shows the crystal structure gradually becoming a vertically oriented 2D structure as the annealing temperature increases.

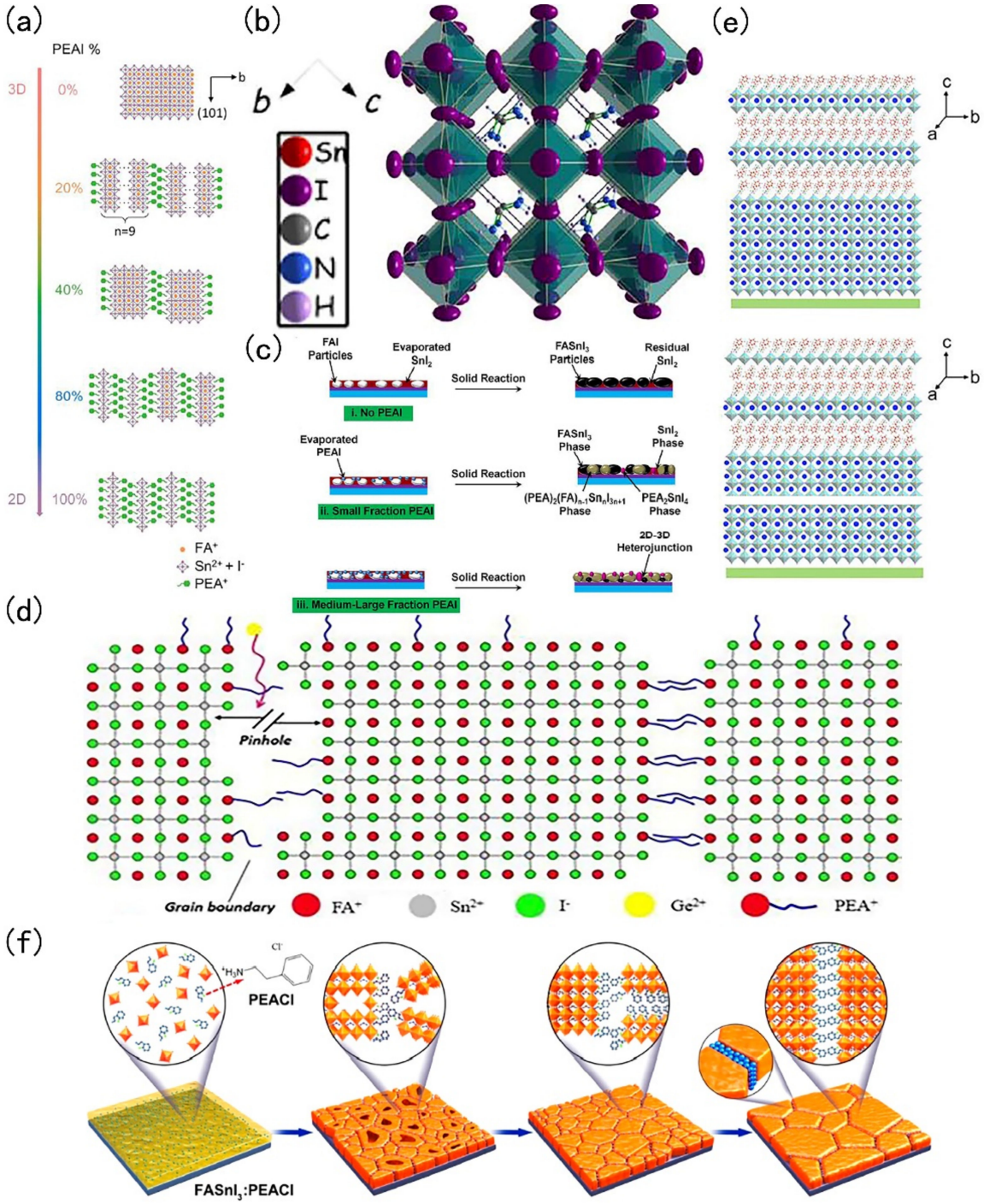

Figure 3. (**a**) As the concentration of PEAI increases, the dimension changes; Letter n denotes the average layers of tin iodide octahedra in nanolayers. Reproduced with permission from [54]. Copyright 2018 American Chemical Society. (**b**) Unit cell and crystal structure of $FASnI_3$ perovskite absorber. Reproduced with permission from [55]. Copyright 2017 The Authors, some rights reserved, exclusive licensee American Association for the Advancement of Science. (**c**) 2D-3D heterojunction production flow chart. Reproduced with permission from [56]. (**d**) Copyright 2018 American Chemical Society. The passivation effect of Ge within the perovskite lattice. Reproduced with permission from [57]. Copyright 2020 The Royal Society of Chemistry. (**e**) Structure characterization of the control film (up) and structure characterization of film with HSP (2D-quasi-2D-3D structure) (down). Reproduced with permission from [58]. Copyright 2018 Elsevier Inc. (**f**) Vertical orientation 2D perovskite structure was attained as the annealing temperature increases. Reproduced with permission from [59]. Copyright 2020 American Chemical Society.

4. Interfacial Layer Engineering

Tin-based perovskite solar cells exist in p-i-n or n-i-p configurations alternating the position of the electron transport (n) and hole transport layer (p). Therefore, during fabrication of these layered devices, it is very common to encounter energy level mismatches and defects at the interface. The simplest trick to improve the performance of tin-based perovskite solar cells is to add an interfacial layer to minimise the energy mismatch and defects at interfaces. Chen and co-workers introduced a low dimension perovskite interlayer. The passivation of defects in perovskite crystals by LDP is shown in Figure 4a. Phenylethyl ammonium bromide (PEABr) was added to a Sn-perovskite absorber layer, then the hole transport layer could separate 3D perovskite crystals into 2D perovskite crystals. The resulting 2D perovskite could greatly reduce the accumulation and recombination of the charge carriers. The manufactured device reaches a PCE of 7.05% [64]. In 2019, Liao and co-workers spin coated PEABr on top of a $FASnI_3$ perovskite layer to form an ultra-thin perovskite layer. After PEABr treatment, the energy level of perovskite, hole transport layer and electron transport layer match well, which was conducive to the better transport of holes and electrons [65]. PEABr changes the perovskite band structure as shown in Figure 4b. Ke and his collaborators spin-coated a ZnS layer on the TiO_2 layer. In this way, the band structure between the electron transport layer and the perovskite layer could be adjusted, and the open circuit voltage could be significantly increased, but the short-circuit current and filling factor were not reduced, and the device achieved a PCE of 5.27% [66]. The energy band diagram of the $FASnI_3$ solar cells and crystal structure of the perovskite absorber are shown in Figure 4c. Hu and his collaborators fabricated SnO_2 and TiO_2 dual-electron transport layer $FASnI_3$ perovskite solar cells. The advantage of this dual-electron transport layer was that it could hinder the formation of defects at the interface and in the perovskite [67]. Song and his collaborators designed a double-layer hole transport layer (CuI and PEDOT: PSS). The 2D double-layer had more outstanding hole-transport capabilities than a single-layer one and it could also improve the quality of perovskite film formation [68]. J-V curve of devices based on various HTLs is shown in Figure 4d. CuI and a PEDOT: PSS double hole transport layer structure change the solar cell stability as shown in Figure 4e.

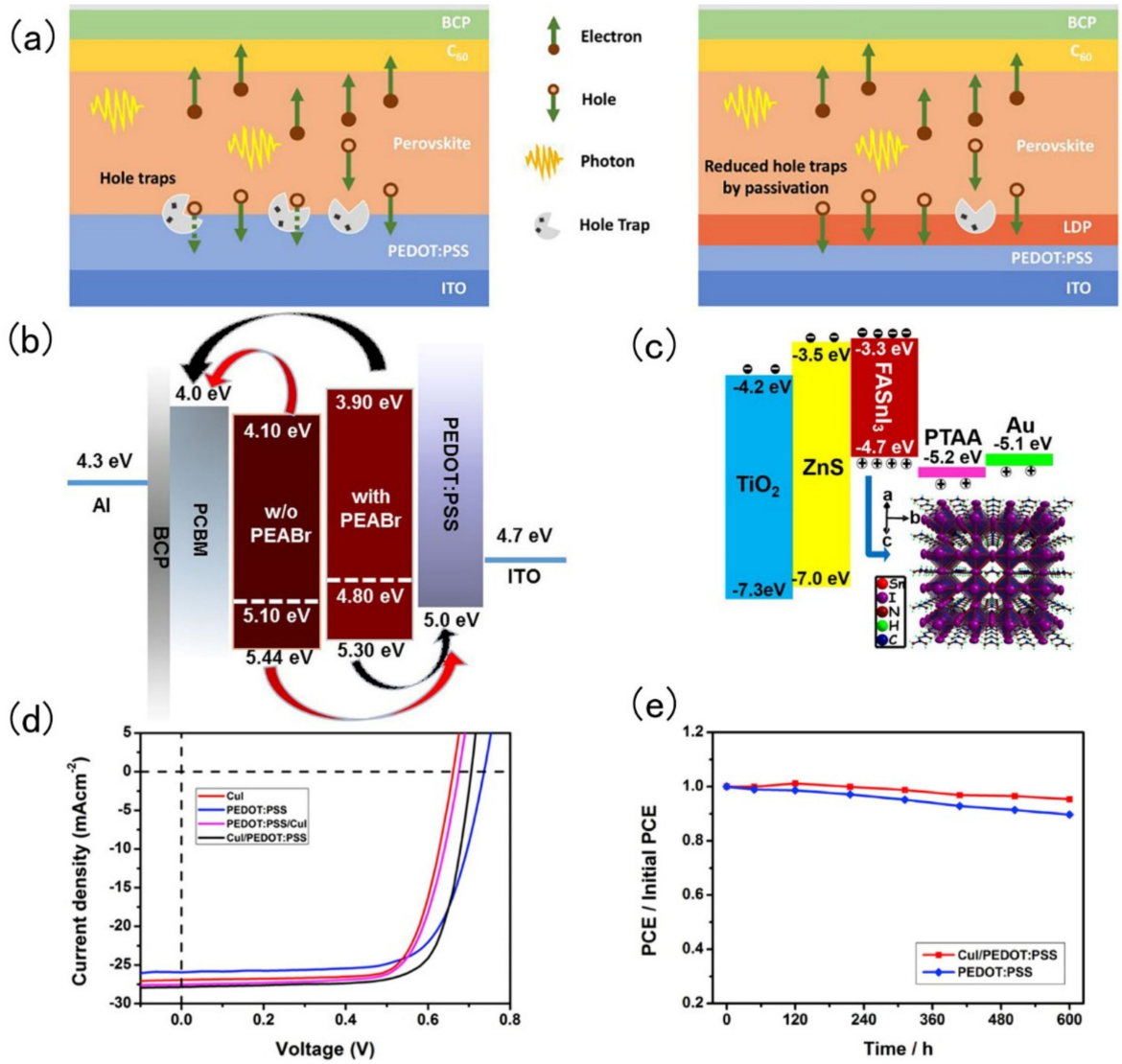

Figure 4. (**a**) Schematic of the trap states reduction by LDP passivation. Reproduced with permission from [64]. Copyright 2018 Elsevier Inc. (**b**) Energy level diagram of the inverted planar PSCs containing $FASnI_3$ without and with PEABr treatment. Reproduced with permission from [65]. Copyright 2019 Wiley-VCH Verlag GmbH & Co. KGaA, Weinheim. (**c**) The energy band diagram of the $FASnI_3$ solar cells and crystal structure of the perovskite absorber. Reproduced with permission from [66] Copyright 2016 American Chemical Society. (**d**) J-V curve of devices based on various HTLs. Reproduced with permission from [68]. Copyright 2020 Elsevier Inc. (**e**) Durability of the unencapsulated devices based on PEDOT: PSS and CuI/PEDOT: PSS HTLs stored in a glovebox for over 600 h. Reproduced with permission from [68]. Copyright 2020 Elsevier Inc.

5. Conclusions and Perspectives

This review briefly introduces the important research progress made in improving the stability and performance of tin-based perovskites. The review focuses on role of introducing additives such as inorganic additives like SnF_2, $NH_4H_2PO_2$, N_2H_5Cl, organic additives, viz. ethylene diammonium diiodide ($EDAI_2$), 5-ammonium valeric acid iodide (5-AVAI) 3-phenyl-2-propen-1-amine (PPA) to study their effects on film properties and device performance. Low-dimensional tin-based perovskites are very mysterious to many researchers and hence it is crucial to understand their properties through in-depth research. This article introduces some tin-based perovskites such as 2D, 3D, 2D-3D, etc. 2D perovskites are more stable than 3D perovskites, but the photoelectric performance is disadvantaged, so low-dimensional perovskite may be a future research hot spot. There will always be

some practical issues in the direct combination of the materials of the tin-based perovskite solar cells. At the same time, it is necessary to add some intermediate layers to solve some discordant factors and improve the performance of the devices. Tin-based perovskite is a promising solar cell material due to its low cost and less toxicity compared with the lead-based perovskite materials, which has encouraged many scientific researchers to work on this type of perovskite. With its interesting features, the instability of tin-based perovskite is also a major problem that needs to be solved to make it commercially viable. Although some work on tin-based perovskites has been done, they are still a long way away from commercialization and considerable work is still needed, for instance, t improves the resistance of tin-based perovskites to match the efficiency of lead-based perovskite solar cells.

Author Contributions: H.L. and Z.Z. contributed equally to this work. H.L. and Z.Z. contributed to methodology, investigation, writing—original draft preparation; F.Y. contributed to validation, data curation, formal analysis; J.Y. contributed to data curation, formal analysis; A.N.G. contributed to data curation, formal analysis; J.L. contributed to validation, data curation, formal analysis; S.T. contributed to data curation, formal analysis; S.M.J. contributed to validation, data curation, formal analysis; All authors have read and agreed to the published version of the manuscript.

Funding: This work was supported by the Henan Province college youth backbone teacher project (No:2020GGJS062); Cultivation Fund for National Scientific Research Project of Henan Normal University (No:2019PL08).

Institutional Review Board Statement: Not applicable.

Informed Consent Statement: Not applicable.

Conflicts of Interest: The authors declare that they had no known competing financial interests or personal relationships that could had appeared to influence the work reported in this paper.

References

1. Kojima, A.; Teshima, K.; Shirai, Y.; Miyasaka, T. Organometal halide perovskites as visible-light sensitizers for photovoltaic cells. *J. Am. Chem. Soc.* **2009**, *131*, 6050–6051. [CrossRef] [PubMed]
2. NREL Efficiency Chart. Available online: https://www.nrel.gov/pv/cell-efficiency.20200406.pdf (accessed on 19 September 2020).
3. Yang, W.F.; Igbari, F.; Lou, Y.H.; Wang, Z.K.; Liao, L.S. Tin halide perovskites: Progress and challenges. *Adv. Energy Mater.* **2019**, *10*, 1902584. [CrossRef]
4. Li, M.; Wang, Z.K.; Zhuo, M.P.; Hu, Y.; Hu, K.H.; Ye, Q.Q.; Jain, S.M.; Yang, Y.G.; Gao, X.Y.; Liao, L.S. Pb–Sn–Cu ternary organometallic halide perovskite solar cells. *Adv. Mater.* **2018**, *30*, e1800258. [CrossRef]
5. Singh, T.; Miyasaka, T. Stabilizing the efficiency beyond 20% with a mixed cation perovskite solar cell fabricated in ambient air under controlled humidity. *Adv. Energy Mater.* **2018**, *8*, 1700677. [CrossRef]
6. Zeng, Q.; Zhang, X.; Feng, X.; Lu, S.; Chen, Z.; Yong, X.; Redfern, S.A.T.; Wei, H.; Wang, H.; Shen, H.; et al.. Polymer-passivated inorganic cesium lead mixed-halide perovskites for stable and efficient solar cells with high open-circuit voltage over 1.3 V. *Adv. Mater.* **2018**, *30*, 1705393. [CrossRef] [PubMed]
7. Valerio, L.; Rosa, A.; Rodriguez, V.; Enriquez, C.; Telles, A.; Ramirez, Y.; Rivera, D.; Hierro, J.; Bustamante, L.; Tong, X.; et al.. Characterization and analysis of $FA_xCs_{(1-x)}$ $Pb(I_yBr_{(1-y)})_3$ perovskite solar cells with thickness controlled transport layers for performance optimization. *AIP Adv.* **2019**, *9*, 105006. [CrossRef]
8. Bai, S.; Da, P.; Li, C.; Wang, Z.; Yuan, Z.; Fu, F.; Kawecki, M.; Liu, X.; Sakai, N.; Wang, J.T.; et al.. Planar perovskite solar cells with long-term stability using ionic liquid additives. *Nature* **2019**, *571*, 245–250. [CrossRef]
9. Li, M.; Yang, Y.G.; Wang, Z.K.; Kang, T.; Wang, Q.; Turren-Cruz, S.H.; Gao, X.Y.; Hsu, C.S.; Liao, L.S.; Abate, A. Perovskite grains embraced in a soft fullerene network make highly efficient flexible solar cells with superior mechanical stability. *Adv. Mater.* **2019**, *31*, e1901519. [CrossRef]
10. Li, M.; Zuo, W.W.; Wang, Q.; Wang, K.L.; Zhuo, M.P.; Köbler, H.; Halbig, C.E.; Eigler, S.; Yang, Y.G.; Gao, X.Y.; et al.. Ultrathin nanosheets of oxo-functionalized graphene inhibit the ion migration in perovskite solar cells. *Adv. Energy Mater.* **2019**, *10*, 1902653. [CrossRef]
11. Zhang, T.; Long, M.; Qin, M.; Lu, X.; Chen, S.; Xie, F.; Gong, L.; Chen, J.; Chu, M.; Miao, Q.; et al.. Stable and efficient 3D-2D perovskite-perovskite planar heterojunction solar cell without organic hole transport layer. *Joule* **2018**, *2*, 2706–2721. [CrossRef]
12. Hartono, N.T.P.; Sun, S.; Gélvez-Rueda, M.C.; Pierone, P.J.; Erodici, M.P.; Yoo, J.; Wei, F.; Bawendi, M.; Grozema, F.C.; Sher, M.-J.; et al.. The effect of structural dimensionality on carrier mobility in lead-halide perovskites. *J. Mater. Chem. A* **2019**, *7*, 23949–23957. [CrossRef]

13. Li, M.; Wang, Z.-K.; Kang, T.; Yang, Y.; Gao, X.; Hsu, C.-S.; Li, Y.; Liao, L.-S. Graphdiyne-modified cross-linkable fullerene as an efficient electron-transporting layer in organometal halide perovskite solar cells. *Nano Energy* **2018**, *43*, 47–54. [CrossRef]
14. Yang, J.; Zhang, Q.; Xu, J.; Liu, H.; Qin, R.; Zhai, H.; Chen, S.; Yuan, M. All-inorganic perovskite solar cells based on $CsPbIBr_2$ and metal oxide transport layers with improved stability. *Nanomaterials* **2019**, *9*, 1666. [CrossRef]
15. Li, J.; Cao, H.L.; Jiao, W.B.; Wang, Q.; Wei, M.; Cantone, I.; Lu, J.; Abate, A. Biological impact of lead from halide perovskites reveals the risk of introducing a safe threshold. *Nat. Commun.* **2020**, *11*, 310. [CrossRef] [PubMed]
16. Shannon, R.D. Revised effective ionic radii and systematic studies of interatomie distances in halides and chaleogenides. *Acta Cryst.* **1976**, *32*, 751. [CrossRef]
17. Noel, N.K.; Stranks, S.D.; Abate, A.; Wehrenfennig, C.; Guarnera, S.; Haghighirad, A.-A.; Sadhanala, A.; Eperon, G.E.; Pathak, S.K.; Johnston, M.B.; et al.. Lead-free organic–inorganic tin halide perovskites for photovoltaic applications. *Energy Environ. Sci.* **2014**, *7*, 3061–3068. [CrossRef]
18. Mare, S.D.; Menossi, D.; Salavei, A.; Artegiani, E.; Piccinelli, F.; Kumar, A.; Mariotto, G.; Romeo, A. SnS thin film solar cells: Perspectives and limitations. *Coatings* **2017**, *7*, 34. [CrossRef]
19. Mare, S.D.; Salavei, A.; Menossi, D.; Piccinelli, F.; Bernardi, P.; Artegiani, E.; Kumar, A.; Mariotto, G.; Romeo, A. A study of SnS recrystallization by post deposition treatment. In Proceedings of the IEEE 43rd Photovoltaic Specialists Conference 2016, Portland, OR, USA, 5–10 June 2016; p. 16468525.
20. Mare, S.D.; Salavei, A.; Menossi, D.; Piccinelli, F.; Artegiani, E.; Kumar, A.; Mariotto, G.; Bernardi, P.; Romeo, A. Effects of temperature and post deposition annealing on SnS polycrystalline thin film growth. In Proceedings of the 32nd European Photovoltaic Solar Energy Conference and Exhibition 2016, Munich, Germany, 20–24 June 2016; pp. 263–266.
21. Takahashi, Y.; Obara, R.; Lin, Z.Z.; Takahashi, Y.; Naito, T.; Inabe, T.; Ishibashi, S.; Terakura, K. Charge-transport in tin-iodide perovskite $CH_3NH_3SnI_3$: Origin of high conductivity. *Dalton Trans.* **2011**, *40*, 5563–5568. [CrossRef]
22. Koh, T.M.; Krishnamoorthy, T.; Yantara, N.; Shi, C.; Leong, W.L.; Boix, P.P.; Grimsdale, A.C.; Mhaisalkar, S.G.; Mathews, N. Formamidinium tin-based perovskite with low E_g for photovoltaic applications. *J. Mater. Chem. A* **2015**, *3*, 14996–15000. [CrossRef]
23. Shi, T.; Zhang, H.-S.; Meng, W.; Teng, Q.; Liu, M.; Yang, X.; Yan, Y.; Yip, H.-L.; Zhao, Y.-J. Effects of organic cations on the defect physics of tin halide perovskites. *J. Mater. Chem. A* **2017**, *5*, 15124–15129. [CrossRef]
24. Bansode, U.; Naphade, R.; Game, O.; Agarkar, S.; Ogale, S. Hybrid Perovskite films by a new variant of pulsed excimer laser deposition: A room-temperature dry process. *J. Phys. Chem. C* **2015**, *119*, 9177–9185. [CrossRef]
25. Song, T.-B.; Yokoyama, T.; Aramaki, S.; Kanatzidis, M.G. Performance enhancement of lead-free tin-based perovskite solar cells with reducing atmosphere-assisted dispersible additive. *ACS Energy Lett.* **2017**, *2*, 897–903. [CrossRef]
26. Lee, S.J.; Shin, S.S.; Kim, Y.C.; Kim, D.; Ahn, T.K.; Noh, J.H.; Seo, J.; Seok, S.I. Fabrication of efficient formamidinium tin iodide perovskite solar cells through SnF_2-pyrazine complex. *J. Am. Chem. Soc.* **2016**, *138*, 3974–3977. [CrossRef]
27. Yokoyama, T.; Song, T.-B.; Cao, D.H.; Stoumpos, C.C.; Aramaki, S.; Kanatzidis, M.G. The origin of lower hole carrier concentration in methylammonium tin halide films grown by a vapor-assisted solution process. *ACS Energy Lett.* **2017**, *2*, 22–28. [CrossRef]
28. Chen, L.J.; Lee, C.R.; Chuang, Y.J.; Wu, Z.H.; Chen, C. Synthesis and optical properties of lead-free cesium tin halide perovskite quantum rods with high-performance solar cell application. *J. Phys. Chem. Lett.* **2016**, *7*, 5028–5035. [CrossRef] [PubMed]
29. Jokar, E.; Chien, C.H.; Tsai, C.M.; Fathi, A.; Diau, E.W. Robust tin-based perovskite solar cells with hybrid organic cations to attain efficiency approaching 10%. *Adv. Mater.* **2019**, *31*, e1804835. [CrossRef]
30. Nishimura, K.; Kamarudin, M.A.; Hirotani, D.; Hamada, K.; Shen, Q.; Iikubo, S.; Minemoto, T.; Yoshino, K.; Hayase, S. Lead-free tin-halide perovskite solar cells with 13% efficiency. *Nano Energy* **2020**, *74*, 104858. [CrossRef]
31. Cao, J.; Tai, Q.; You, P.; Tang, G.; Wang, T.; Wang, N.; Yan, F. Enhanced performance of tin-based perovskite solar cells induced by an ammonium hypophosphite additive. *J. Mater. Chem. A* **2019**, *7*, 26580–26585. [CrossRef]
32. Tai, Q.; Guo, X.; Tang, G.; You, P.; Ng, T.W.; Shen, D.; Cao, J.; Liu, C.K.; Wang, N.; Zhu, Y.; et al.. Antioxidant grain passivation for air-stable tin-based perovskite solar cells. *Angew. Chem. Int. Ed. Engl.* **2019**, *58*, 806–810. [CrossRef]
33. Kayesh, M.E.; Chowdhury, T.H.; Matsuishi, K.; Kaneko, R.; Kazaoui, S.; Lee, J.-J.; Noda, T.; Islam, A. Enhanced photovoltaic performance of FASnI3-based perovskite solar cells with hydrazinium chloride coadditive. *ACS Energy Lett.* **2018**, *3*, 1584–1589. [CrossRef]
34. Chung, I.; Lee, B.; He, J.; Chang, R.P.; Kanatzidis, M.G. All-solid-state dye-sensitized solar cells with high efficiency. *Nature* **2012**, *485*, 486–489. [CrossRef]
35. Kumar, M.H.; Dharani, S.; Leong, W.L.; Boix, P.P.; Prabhakar, R.R.; Baikie, T.; Shi, C.; Ding, H.; Ramesh, R.; Asta, M.; et al.. Lead-free halide perovskite solar cells with high photocurrents realized through vacancy modulation. *Adv. Mater.* **2014**, *26*, 7122–7127. [CrossRef] [PubMed]
36. Hao, F.; Stoumpos, C.C.; Guo, P.; Zhou, N.; Marks, T.J.; Chang, R.P.; Kanatzidis, M.G. Solvent-mediated crystallization of $CH_3NH_3SnI_3$ films for heterojunction depleted perovskite solar cells. *J. Am. Chem. Soc.* **2015**, *137*, 11445–11452. [CrossRef]
37. Liao, W.; Zhao, D.; Yu, Y.; Grice, C.R.; Wang, C.; Cimaroli, A.J.; Schulz, P.; Meng, W.; Zhu, K.; Xiong, R.G.; et al.. Lead-free inverted planar formamidinium tin triiodide perovskite solar cells achieving power conversion efficiencies up to 6.22%. *Adv. Mater.* **2016**, *28*, 9333–9340. [CrossRef] [PubMed]
38. Ma, L.; Hao, F.; Stoumpos, C.C.; Phelan, B.T.; Wasielewski, M.R.; Kanatzidis, M.G. Carrier diffusion lengths of over 500 nm in lead-free perovskite $CH_3NH_3SnI_3$ films. *J. Am. Chem. Soc.* **2016**, *138*, 14750–14755. [CrossRef] [PubMed]

39. Handa, T.; Yamada, T.; Kubota, H.; Ise, S.; Miyamoto, Y.; Kanemitsu, Y. Photocarrier recombination and injection dynamics in long-term stable lead-free $CH_3NH_3SnI_3$ perovskite thin films and solar cells. *J. Phys. Chem. C* **2017**, *121*, 16158–16165. [CrossRef]
40. Milot, R.L.; Klug, M.T.; Davies, C.L.; Wang, Z.; Kraus, H.; Snaith, H.J.; Johnston, M.B.; Herz, L.M. The effects of doping density and temperature on the optoelectronic properties of formamidinium tin triiodide thin films. *Adv. Mater.* **2018**, *30*, e1804506. [CrossRef]
41. Hartmann, C.; Gupta, S.; Bendikov, T.; Kozina, X.; Kunze, T.; Félix, R.; Hodes, G.; Wilks, R.G.; Cahen, D.; Bär, M. Interfaces, impact of SnF_2 addition on the chemical and electronic surface structure of $CsSnBr_3$. *ACS Appl. Mater. Interfaces* **2020**, *12*, 12353–12361. [CrossRef] [PubMed]
42. Gao, W.; Ran, C.; Li, J.; Dong, H.; Jiao, B.; Zhang, L.; Lan, X.; Hou, X.; Wu, Z. Robust stability of efficient lead-free formamidinium tin iodide perovskite solar cells realized by structural regulation. *J. Phys. Chem. Lett.* **2018**, *9*, 6999–7006. [CrossRef] [PubMed]
43. Ke, W.; Stoumpos, C.C.; Spanopoulos, I.; Chen, M.; Wasielewski, M.R.; Kanatzidis, M.G. Diammonium cations in the $FASnI_3$ perovskite structure lead to lower dark currents and more efficient solar cells. *ACS Energy Lett.* **2018**, *3*, 1470–1476. [CrossRef]
44. Jokar, E.; Chien, C.-H.; Fathi, A.; Rameez, M.; Chang, Y.-H.; Diau, E.W.-G. Slow surface passivation and crystal relaxation with additives to improve device performance and durability for tin-based perovskite solar cells. *Energy Environ. Sci.* **2018**, *11*, 2353–2362. [CrossRef]
45. Kayesh, M.E.; Matsuishi, K.; Kaneko, R.; Kazaoui, S.; Lee, J.-J.; Noda, T.; Islam, A. Coadditive engineering with 5-ammonium valeric acid iodide for efficient and stable sn perovskite solar cells. *ACS Energy Lett.* **2018**, *4*, 278–284. [CrossRef]
46. Ran, C.; Gao, W.; Li, J.; Xi, J.; Li, L.; Dai, J.; Yang, Y.; Gao, X.; Dong, H.; Jiao, B.; et al.. Conjugated organic cations enable efficient self-healing FASnI3 solar cells. *Joule* **2019**, *3*, 3072–3087. [CrossRef]
47. Yu, B.B.; Xu, L.; Liao, M.; Wu, Y.; Liu, F.; He, Z.; Ding, J.; Chen, W.; Tu, B.; Lin, Y.; et al.. Synergy effect of both 2,2,2-trifluoroethylamine hydrochloride and SnF_2 for highly stable $FASnI_{3-x}Cl_x$ perovskite solar cells. *Solar RRL* **2019**, *3*, 1800290. [CrossRef]
48. He, X.; Wu, T.; Liu, X.; Wang, Y.; Meng, X.; Wu, J.; Noda, T.; Yang, X.; Moritomo, Y.; Segawa, H.; et al.. Highly efficient tin perovskite solar cells achieved in a wide oxygen concentration range. *J. Mater. Chem. A* **2020**, *8*, 2760–2768. [CrossRef]
49. Boehm, A.M.; Liu, T.; Park, S.M.; Abtahi, A.; Graham, K.R. Influence of surface ligands on energetics at $FASnI_3$/C60 interfaces and their impact on photovoltaic performance. *ACS Appl. Mater. Interfaces* **2020**, *12*, 5209–5218. [CrossRef]
50. Zeng, W.; Cui, D.; Li, Z.; Tang, Y.; Yu, X.; Li, Y.; Deng, Y.; Ye, R.; Niu, Q.; Xia, R.; et al.. Surface optimization by poly(α-methylstyrene) as additive in the anti-solution to enhance lead-free Sn-based perovskite solar cells. *Sol. Energy* **2019**, *194*, 272–278. [CrossRef]
51. Meng, X.; Lin, J.; Liu, X.; He, X.; Wang, Y.; Noda, T.; Wu, T.; Yang, X.; Han, L. Highly stable and efficient FASnI3-based perovskite solar cells by introducing hydrogen bonding. *Adv. Mater.* **2019**, *31*, e1903721. [CrossRef]
52. Lin, Z.; Liu, C.; Liu, G.; Yang, J.; Duan, X.; Tan, L.; Chen, Y. Preparation of efficient inverted tin-based perovskite solar cells via the bidentate coordination effect of 8-hydroxyquinoline. *Chem. Commun.* **2020**, *56*, 4006–4010. [CrossRef]
53. Wu, T.; Liu, X.; He, X.; Wang, Y.; Meng, X.; Noda, T.; Yang, X.; Han, L. Efficient and stable tin-based perovskite solar cells by introducing π-conjugated Lewis base. *Sci. China Chem.* **2019**, *63*, 107–115. [CrossRef]
54. Liao, Y.; Liu, H.; Zhou, W.; Yang, D.; Shang, Y.; Shi, Z.; Li, B.; Jiang, X.; Zhang, L.; Quan, L.N.; et al.. Highly oriented low-dimensional tin halide perovskites with enhanced stability and photovoltaic performance. *J. Am. Chem. Soc.* **2017**, *139*, 6693–6699. [CrossRef]
55. Ke, W.; Stoumpos, C.C.; Zhu, M.; Mao, L.; Spanopoulos, I.; Liu, J.; Kontsevoi, O.Y.; Chen, M.; Sarma, D.; Zhang, Y.; et al.. Enhanced photovoltaic performance and stability with a new type of hollow 3D perovskite {en}$FASnI_3$. *Sci. Adv.* **2017**, *3*, e1701293. [CrossRef] [PubMed]
56. Ran, C.; Xi, J.; Gao, W.; Yuan, F.; Lei, T.; Jiao, B.; Hou, X.; Wu, Z. Bilateral interface engineering toward efficient 2D–3D bulk heterojunction tin halide lead-free perovskite solar cells. *ACS Energy Lett.* **2018**, *3*, 713–721. [CrossRef]
57. Ng, C.H.; Hamada, K.; Kapil, G.; Kamarudin, M.A.; Wang, Z.; Iikubo, S.; Shen, Q.; Yoshino, K.; Minemoto, T.; Hayase, S. Reducing Traps Density and Carriers Concentration by Ge Additive for An Efficient Quasi 2D/3D Perovskite Solar Cell. *J. Mater. Chem. A* **2020**, *8*, 2962–2968. [CrossRef]
58. Wang, F.; Jiang, X.; Chen, H.; Shang, Y.; Liu, H.; Wei, J.; Zhou, W.; He, H.; Liu, W.; Ning, Z. 2D-quasi-2D-3D hierarchy structure for tin perovskite solar cells with enhanced efficiency and stability. *Joule* **2018**, *2*, 2732–2743. [CrossRef]
59. Li, M.; Zuo, W.-W.; Yang, Y.-G.; Aldamasy, M.H.; Wang, Q.; Cruz, S.H.T.; Feng, S.-L.; Saliba, M.; Wang, Z.-K.; Abate, A. Tin halide perovskite films made of highly oriented 2D crystals enable more efficient and stable lead-free perovskite solar cells. *ACS Energy Lett.* **2020**, *5*, 1923–1929. [CrossRef]
60. Xu, H.; Jiang, Y.; He, T.; Li, S.; Wang, H.; Chen, Y.; Yuan, M.; Chen, J. Orientation regulation of tin-based reduced-dimensional perovskites for highly efficient and stable photovoltaics. *Adv. Funct. Mater.* **2019**, *29*, 1907696. [CrossRef]
61. Tsai, C.-M.; Lin, Y.-P.; Pola, M.K.; Narra, S.; Jokar, E.; Yang, Y.-W.; Diau, E.W.-G. Control of crystal structures and optical properties with hybrid formamidinium and 2-hydroxyethylammonium cations for mesoscopic carbon-electrode tin-based perovskite solar cells. *ACS Energy Lett.* **2018**, *3*, 2077–2085. [CrossRef]
62. Li, P.; Liu, X.; Zhang, Y.; Liang, C.; Chen, G.; Li, F.; Su, M.; Xing, G.; Tao, X.; Song, Y. Low-dimensional dion–jacobson-phase lead-free perovskites for high-performance photovoltaics with improved stability. *Angew. Chem. Int. Ed. Engl.* **2020**, *59*, 6909–6914. [CrossRef] [PubMed]

63. Chen, A.Z.; Shiu, M.; Ma, J.H.; Alpert, M.R.; Zhang, D.; Foley, B.J.; Smilgies, D.M.; Lee, S.H.; Choi, J.J. Origin of vertical orientation in two-dimensional metal halide perovskites and its effect on photovoltaic performance. *Nat. Commun.* **2018**, *9*, 1336. [CrossRef]
64. Chen, K.; Wu, P.; Yang, W.; Su, R.; Luo, D.; Yang, X.; Tu, Y.; Zhu, R.; Gong, Q. Low-dimensional perovskite interlayer for highly efficient lead-free formamidinium tin iodide perovskite solar cells. *Nano Energy* **2018**, *49*, 411–418. [CrossRef]
65. Liao, M.; Yu, B.B.; Jin, Z.; Chen, W.; Zhu, Y.; Zhang, X.; Yao, W.; Duan, T.; Djerdj, I.; He, Z. Efficient and stable $FASnI_3$ perovskite solar cells with effective interface modulation by low-dimensional perovskite layer. *ChemSusChem* **2019**, *12*, 5007–5014. [CrossRef] [PubMed]
66. Ke, W.; Stoumpos, C.C.; Logsdon, J.L.; Wasielewski, M.R.; Yan, Y.; Fang, G.; Kanatzidis, M.G. TiO_2-ZnS cascade electron transport layer for efficient formamidinium tin iodide perovskite solar cells. *J. Am. Chem. Soc.* **2016**, *138*, 14998–15003. [CrossRef] [PubMed]
67. Hu, M.; Zhang, L.; She, S.; Wu, J.; Zhou, X.; Li, X.; Wang, D.; Miao, J.; Mi, G.; Chen, H.; et al.. Electron transporting bilayer of SnO_2 and TiO_2 nanocolloid enables highly efficient planar perovskite solar cells. *Solar RRL* **2019**, *4*, 1900331. [CrossRef]
68. Song, J.; Hu, W.; Li, Z.; Wang, X.-F.; Tian, W. A double hole-transport layer strategy toward efficient mixed tin-lead iodide perovskite solar cell. *Sol. Energy Mater. Sol. Cells* **2020**, *207*, 110351. [CrossRef]